Comparison of optimised conditions for inductively coupled plasma-reactive ion etching of quartz substrates and its optical applications

Yu-Hsiang Tang, Yu-Hsin Lin, Po-Li Chen, Ming-Hua Shiao, Chien-Nan Hsiao

National Applied Research Laboratories, Instrument Technology Research Center, Hsinchu 300, Taiwan
E-mail: sky520830@itrc.narl.org.tw

Published in Micro & Nano Letters; Received on 19th February 2014; Revised on 9th April 2014; Accepted on 13th May 2014

A C_4F_8/He inductively coupled plasma-reactive ion etching (ICP-RIE) was studied to improve the etching conditions of quartz glass. The influences of C_4F_8 flow rate, He flow rate, chamber pressure, inductively coupled plasma (ICP) power, bias power and cooling temperature were investigated. A report is presented on an optimum etching condition for fabricating quartz-based optical components considering their application in diffractive optical element (DOE) devices. As per these etching results, the etched microstructure exhibited a depth of 44.2 μm and a vertical sidewall angle of 89° resulting from an ICP power of 3000 W, a bias power of 200 W, a chamber pressure of 2.5 mTorr and an etching time of 120 min in a mixture of C_4F_8 and He gases with 30 and 100 sccm flow rates, respectively. The successful fabrication of the DOE component by ICP-RIE is reported. This can be used to provide the uniform light intensity distribution for a DOE device.

1. Introduction: Glass microstructures have been widely used in many device applications for microelectromechanical systems (MEMS) [1, 2], optical devices [3, 4] and biomedical chips [5, 6]. The commonly used glass substrates, such as silica [7], borosilicate glass [8], Corning Pyrex 7740 glass [9] and quartz glass [10], possess several significant properties such as excellent optical transmission, low resistance and high biocompatibility and so on [11, 12]. Quartz glass, which exhibits piezoelectricity, insulation, optical transparency, hardness and thermal stability, is one of the potential materials that can be used to develop optical components [13, 14].

The enormous difficulties in developing MEMS on quartz substrates are the low etch rate, and fabrication of a high-aspect-ratio structure process, which is related to charge accumulation, plasma density and gas transfer rates. With microcomponent size scaling down as a result of modern research developments, the requirements of smaller linewidth in processing, anisotropy and selectivity are increasingly strict. In nanoengineering and MEMS, the vertical trench structure fabricated on quartz substrates is the key technology. Several microfabrication methods have been reported for etching quartz glass, such as laser milling, drilling and powder blasting. However, these conventional micromachining techniques cannot easily fabricate appropriately nanostructure and microstructure ranges on quartz glass. Chemical wet [15, 16] and dry etching [17, 18] are the two methods most efficiently used to etch quartz glass. Wet etching adopts an HF solution to improve the etching ratio in different lattice directions on glass substrates. The advantage of wet etching is that it exhibits a very high etching selectivity for the glass and mask materials. The disadvantages of wet etching are undercut and isotropic etching (same etching ratio in each direction), which greatly restricts the structural shape. In etching technology, MEMS usually require vertical and planar structures. Dry etching provides many more advantages than wet etching, such as an improved etching ratio control, precise etching size, sidewall verticality and high-aspect-ratio structures.

Several dry etching systems with high-density plasma sources including inductively coupled plasma (ICP) [19], electron cyclotron resonance [20] and capacitively coupled plasma [21] have been reported to etch glass substrates. Among them, ICP-reactive ion etching (ICP-RIE), because of its anisotropic, dimensional precision and high-aspect-ratio properties were attractively utilised for the microfabrication of quartz substrate. The primary challenge in the dry etching of glass is to produce high-energy ions to break Si–O bonds. ICP-RIE generating various fluorine-based plasmas with different gases such as C_4F_8 [22], CHF_3 [23], SF_6 [24], SF_6/Ar [25], C_4F_8/O_2 and C_4F_8/He [26] have been studied previously for quartz glass etching and manifest deep trench structures.

However, the ICP-RIE of quartz glass etching has several problems such as slow etch rate, low etch selectivity to masking material, surface roughness and sidewall angle. Therefore a determining process to optimise experimental parameters has become an important issue for quartz glass etching with ICP-RIE technology.

In this Letter, we present the details of the ICP-RIE process to examine the etching characteristics of quartz glass. We also explore the influence of the etching parameters (gas flow, gas composition, chamber pressure, ICP power and bias power) on the surface profile, etching rate and sidewall verticality to determine the optimum etching conditions. Moreover, we present an optimised etching parameter for the application to DOE devices.

2. Experimental description and procedure: Fig. 1*a* shows a schematic diagram of the ICP-RIE (Plasmalab System 100 ICP380, Oxford Instruments) used for microtrench etching in this study. High-density plasmas were generated by an RF power applied to the ICP source (up to 5000 W) and extracted using an RF power applied to the substrate electrode (up to 500 W). It is provided with a commercial Oxford ICP source at 13.56 MHz. The mechanism of quartz glass etching in this system comprises multiple steps. First, positive ions are introduced to break the Si–O bonds. Afterwards, C_xF_y polymer films are continuously deposited on the substrate. Heavier ions collide in the layer located between the deposited C_xF_y and SiO_2 layers, producing the etching reaction as shown in Fig. 1*b* [27, 28].

The process of quartz glass etching consumes fluorine atoms, combining them with silicon atoms to form SiF_x gas, which readily evaporates. However, the discharged oxygen reacts with CF_x radicals in quartz glass etching to form CO, CO_2 and COF_2, which readily evaporate [29]. Hence, the chemical deposition accelerates ion bombardment and results in anisotropic etching.

A scanning electron microscope (SEM; Hitachi S-4300) and white light interferometer (ZYGO; NewView™ 5100) were employed to observe the micrographs of the quartz glass generated by the etching process and the experimental results are now discussed.

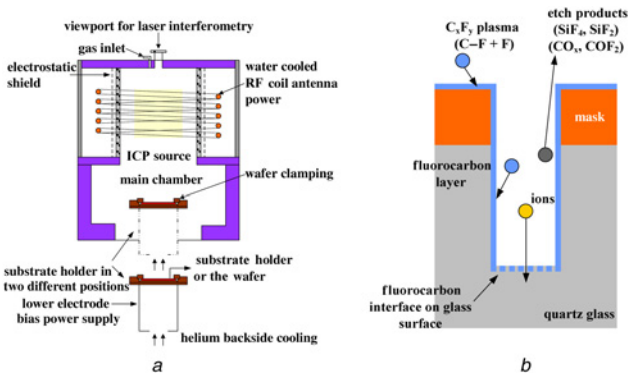

Figure 1 *Schematic of dry etching equipment for etching quartz glass (model: Oxford Plasma Lab 100 System with ICP 380 source) (Fig. 1a), and etching mechanism of quartz glass with C_4F_8 (Fig. 1b)*

3. Experimental results: Fig. 2 shows the detailed process characterisation performed by varying the process parameters. These standard parameters included C_4F_8 flow rate (12 sccm), He flow rate (84 sccm), chamber pressure (10 mTorr), ICP power (1500 W), bias power (120 W) and cooling temperature (2.5°C). In each case, the main factor was varied with the etching time for 30 min, while all other variables were held at optimum values.

3.1. Influence of C_4F_8/He gas flow rate: Fig. 2*a* shows the relationship between C_4F_8 gas flow rate and the etching depth and etching rate. As shown in Fig. 2*a*, when the C_4F_8 gas flow rate increases from 5 to 30 sccm, the etching depth increases from 5.9 to 9.7 μm and the etching rate increases from 177 to 323 nm/min. Fig. 2*b* shows the relationship between He gas flow rate and etching depth and etching rate. As shown in Fig. 2*b*, as the He gas flow rate increases from 20 to 100 sccm, the etching depth increases from 6.7 to 8.6 μm and the etching rate increases from 223 to 287 nm/min. The etching rate proportionally increases as the gas-flow rate increases.

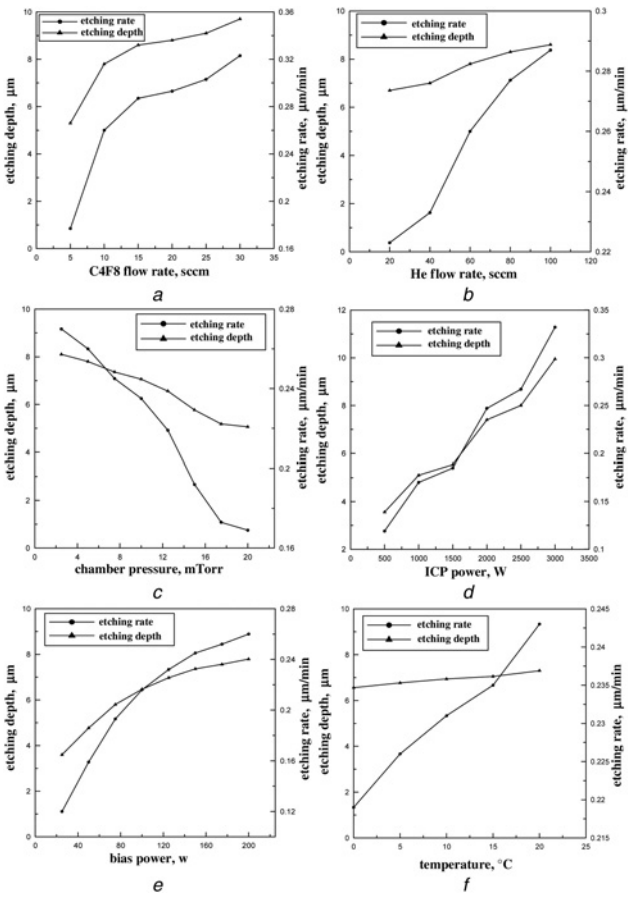

Figure 2 *Measured etching rate and etching depth against C_4F_8 flow rate (Fig. 2a), He flow rate (Fig. 2b), chamber pressure (Fig. 2c), ICP power (Fig. 2d), bias power (Fig. 2e), cooling temperature (Fig. 2f)*

3.2. Influence of chamber pressure: Fig. 2*c* shows the relationship between chamber pressure and both the etching depth and rate. As the chamber pressure increases from 2.5 to 20 mTorr, the etching depth decreases from 8.1 to 5.06 μm and the etching rate decreases from 270 to 169 nm/min.

The experiment indicated that the chamber pressure and etching rate were in inversely proportional relationship. C_4F_8/He gas flow rate and etching rate were related proportionally. The etching rate did not increase as the gas pressure and He gas flow rate were changed. This means that the C_4F_8 gas flow rate is the main factor that affects the quartz etching rate. Besides, C_4F_8 gas is better at controlling the dimensions and etching rate of structures.

3.3. Influence of ICP/bias power: Fig. 2*d* shows the relationship between ICP power and the etching depth and rate. As the ICP power increases from 500 to 3000 W, the etching depth increases from 3.6 to 9.9 μm and the etching rate increases from 119 to 332 nm/min. The curve in Fig. 2*d* also shows that as the ICP power increases, plasma density increases. This results in an increased efficiency for C_4F_8/He gas molecule dissociation and ionisation. Thus, chemical etching accelerates the breakage of Si–O bonds.

Fig. 2*e* shows the relationship between bias power and the etching depth and etching rate. As bias power increases from 25 to 200 W, the etching depth increases from 3.6 to 7.8 μm and the etching rate increases from 120 to 260 nm/min. These results indicate that higher bias power causes higher DC bias. A high F ion energy and the fast removal of SiF product increase the ionic bombardment and bond breakage efficiencies. Thus, the etching rate proportionally increases as the ICP/bias power increases.

3.4. Influence of substrate temperature: Fig. 2*f* shows the relationship between the substrate temperature and the etching depth and the etching rate. As the etching temperature increases from 0 to 20°C, the etching depth increases from 6.6 to 7.3 μm and the etching rate increases from 219 to 243 nm/min. The curve in Fig. 2*f* also shows that as the temperature increases the etching rate slightly improves. This is because rising temperature can increase the kinetic energy of the reaction of the oxidation layer.

In the investigation of the effect of the substrate temperature on the etching rate, it was found that temperature factors include chiller and backside helium cooling. The thermal contact mainly occurred between the glass and aluminium substrate of the bottom electrode. When the etching time was greater than 30 min, the substrate temperature started rising. Thus, the etching rate slightly increased, but not to a significant level.

A comparison of the etching rates in Figs. 2*a* and *d* indicates that the C_4F_8 flow rate and ICP power are the key parameters determining the etching rate. Thus, to obtain a high etching rate, low surface roughness and vertical sidewall morphology, low chamber pressure, high gas flow rate, high ICP power and high bias power are critical for adjusting these parameters. The etching parameters are indeed consistent with the uniformity of the process. It was found that plasma density, fluorine gas dissociation and ionic bombardment energy were the main factors affecting the etching rate.

On the basis of the above investigation and the effects of different etching process parameters, the optimal parameters were selected to fabricate the trench structure. To optimally fabricate the trench, an ICP power of 3000 W, a bias power of 200 W, a chamber pressure of 2.5 mTorr, a C_4F_8/He flow rate of 30/100 sccm and an etching

doi: 10.1049/mnl.2014.0093

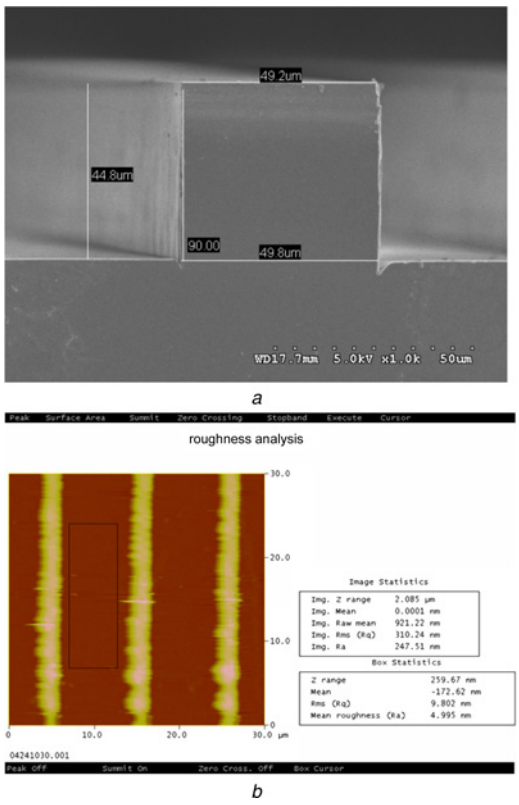

Figure 3 *Micrographs, obtained using SEM and atomic force microscope, of microtrench structures of quartz glass after C_4F_8/He plasma etching with etching mask of negative photoresist (KMPR 1050)*
a Side view of quartz glass with sidewall vertical angle of 89°
b Roughness of etched surface was 4.995 nm

time of 120 min were used. Fig. 3*a* shows the cross-sectional view of the microtrench structures after the ICP-RIE process. We obtained a sidewall verticality of 89°, an etching depth of ~44.6 µm, an etching rate of 0.358 µm/min and a depth uniformity within 4%. Fig. 3*b* shows the etched bottom roughness of ~4.995 nm.

3.5. Fabrication of quartz DOE optical devices: The development of the deep etching process for quartz glass can improve the design, fabrication and testing of microoptic components. These components have applications in micrograting, diffractive optical element (DOE) devices, nanostructures, three-dimensional (3D)-packages and bio-MEMS. In the following paragraphs, we will focus on the DOE device to describe the application of dry etching in optical device systems.

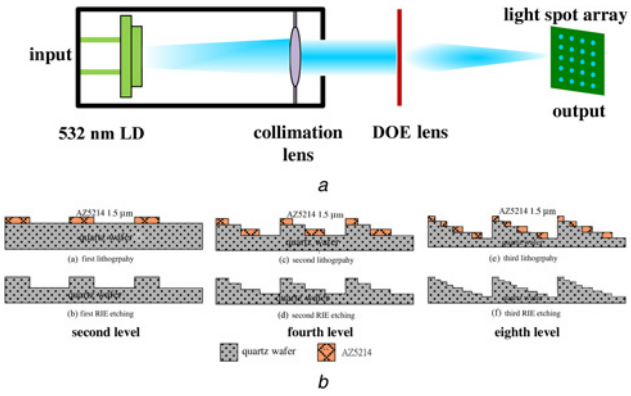

Figure 4 *Illustration of eighth-level DOE device (Fig. 4a), and six-step fabrication process for eighth-level optical device using lithography and ICP-RIE process (Fig. 4b)*

The objective was to develop an optical device that can produce a multi-light spot array as a special diffractive optical device, as shown in Fig. 4*a*. A laser with a wavelength of 532 nm was used as a source. After collimation, it formed a square planar beam (7.5 × 7.5 mm) incident on the fabricated optical device, which could generate the required light spot array on a specific location in a certain distance from the device. Subsequently, a scan projection optical system was used to project the generated light spot array onto a chip to produce a hole array on a target wafer.

Fig. 4*b* illustrates a six-step fabrication process for patterning the DOE devices on quartz glass. An eighth-level surface profile is formed by repeating the photolithography and ICP-RIE fabrication steps. First, a positive photoresist (AZ5214) was spin coated by a spinner and patterned by photolithography, then transferred by etching process. We obtained a second-level DOE shape that was transferred to a quartz glass; also the fourth-level and eighth-level DOE are repetitions of the above-mentioned process. The depth of etchings done using the three-mask process was designed to be 0.66247, 0.32417 and 0.164964 µm. Fig. 5 shows a white light

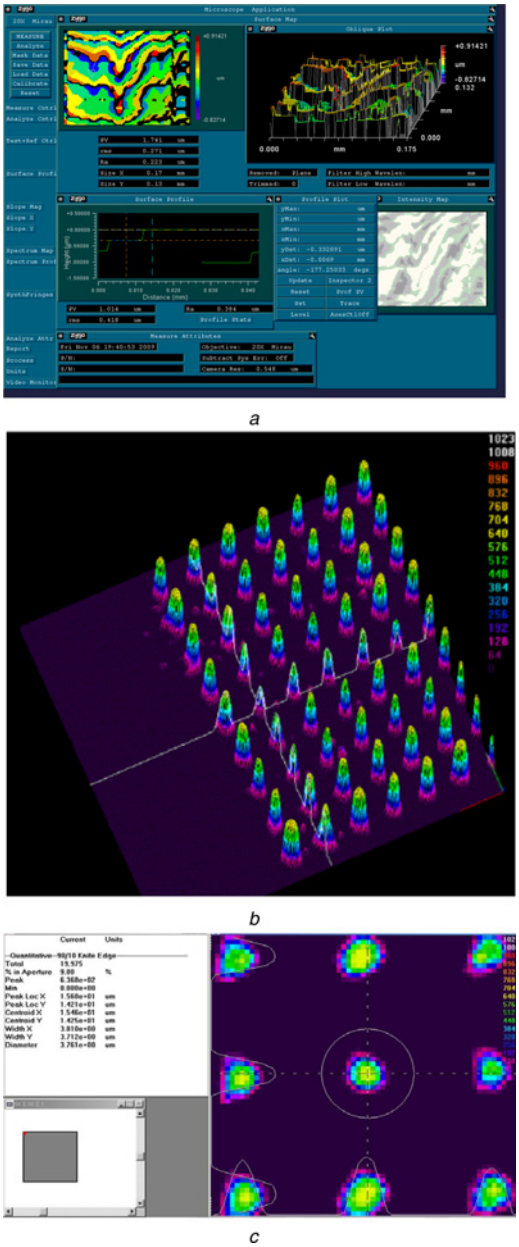

Figure 5 *Surface profile of optical element measured using white light interferometer (Fig. 5a); measurement illustrates light intensity distribution of focal plane and diameter of light spots (Figs. 5b and c)*

interferometer image of an etched profile of quartz glass for a DOE device. The etched depths of 0.332891 μm were measured using a white-light interferometer, as shown in Fig. 5*a*. The fabrication process resulted in an error of 3–5% in the etched depth. Fig. 5*b* shows the 3D light distribution diagram for the device on a focal plane. Measurements demonstrated that the fabricated DOE has the desired function and has uniform light intensity. The energy magnitude shows that the light spot size is reduced to 13.5% of the original peak value, as shown in Fig. 5*c*. The diameter of the transverse light spots was 3.81 μm. The diameter of the longitudinal light spots was 3.71 μm.

4. Conclusion: In this Letter, we report the characteristics of the ICP-RIE of quartz glass in C_4F_8/He plasma. The optimisation of etching rate (~0.358 μm/min), etched depth (~11.3 μm), side-wall angle (~89°) and the smooth surface (roughness of ~4.995 nm) were achieved at the optimum conditions of ICP power (3000 W), bias power (200 W), process pressure (2.5 mTorr), C_4F_8 (30 sccm) and He (100 sccm). Consequently, these parameters were successfully applied in the DOE device fabrication, and it was shown that ICP-RIE can be used to realise a uniform light intensity distribution. In addition, the measurement error of the etched depth and the light spot size for the optical device was within 3–5% and reduced to 13.5%, respectively.

5 References

[1] Zeze D.A., Forrest R.D., Carey J.D., *ET AL.*: 'Reactive ion etching of quartz and Pyrex for microelectronic applications', *J. Appl. Phys.*, 2002, **92**, pp. 3624–3629

[2] Esashi M., Takinami M., Wakabayashi Y., Minami K.: 'High-rate directional deep dry etching for bulk silicon micromachining', *J. Micromech. Microeng.*, 1995, **5**, pp. 5–10

[3] Mohamed K., Alkaisi M.M., Blaikie R.J.: 'Fabrication of three dimensional structures for an UV curable nanoimprint lithography mold using variable dose control with critical-energy electron beam exposure', *J. Vac. Sci. Technol. B*, 2007, **25**, pp. 2357–2360

[4] Wang S., Zhou C., Ru H., Zhang Y.: 'Optimized condition for etching fused-silica phase gratings with inductively coupled plasma technology', *Appl. Opt.*, 2005, **44**, pp. 4429–4434

[5] Ujiie T., Kikuchi T., Ichiki T., Horiike Y.: 'Fabrication of quartz microcapillary electrophoresis chips using plasma etching', *Jpn. J. Appl. Phys.*, 2000, **39**, pp. 3677–3682

[6] Tathagata R., Haixin Z., Deirdre R.M.: 'Deep reactive ion etching of fused silica using a single-coated soft mask layer for bio-analytical applications', *J. Micromech. Microeng.*, 2010, **20**, p. 097002

[7] Rabe J., Buttgenbach S., Schroder J., Hauptmann P.: 'Monolithic miniaturized quartz microbalance array and its application to chemical sensor systems for liquids', *IEEE Sens. J.*, 2003, **3**, pp. 361–368

[8] Park J.H., Lee N.E., Lee J., Park J.S., Park H.D.: 'Deep dry etching of borosilicate glass using SF_6 and SF_6/Ar inductively coupled plasmas', *Microelecron. Eng.*, 2005, **82**, pp. 119–128

[9] Ok S.J., Kim C., Baldwin D.F.: 'High density, high aspect ratio through-wafer electrical interconnect vias for MEMS packaging', *IEEE Trans. Adv. Packag.*, 2003, **26**, pp. 302–309

[10] Abe T., Esashi M.: 'One-chip multichannel quartz crystal microbalance (QCM) fabricated by deep RIE', *Sens. Actuators A*, 2000, **82**, pp. 139–143

[11] Lilienthal K., Stubenrauch M., Fischer M., Schober A.: 'Fused silica 'glass grass': fabrication and utilization', *J. Micromech. Microeng.*, 2010, **20**, p. 025017

[12] Akashi T., Yoshimura Y.: 'Deep reactive ion etching of borosilicate "glass using" an anodically bonded silicon wafer as an etching mask', *J. Micromech. Microeng.*, 2006, **16**, pp. 1051–1056

[13] Morikawa Y., Koidesawa T., Hayashi T., Suu K.: 'A novel deep etching technology for Si and quartz materials', *Thin Solid Films*, 2007, **515**, pp. 4918–4922

[14] Zhu H., Holl M., Ray T., Bhushan S., Meldrum D.R.: 'Characterization of deep wet etching of fused silica glass for single cell and optical sensor deposition', *J. Micromech. Microeng.*, 2009, **19**, p. 065013

[15] Stjernstrom M., Roeraade J.: 'Method for fabrication of microfluidic systems in glass', *J. Micromech. Microeng.*, 1998, **8**, pp. 33–38

[16] Hedlund C., Lindberg U., Bucht U., Soderkvist J.: 'Anisotropic etching of Z-cut quartz', *J. Micromech. Microeng.*, 1993, **3**, pp. 65–73

[17] Lopez A.G., Craighead H.G.: 'Subwavelength surface-relief gratings fabricated by microcontact printing of self-assembled monolayers', *Appl. Opt.*, 2001, **40**, pp. 2068–2075

[18] Clausnitzer T., Limpert J., Zöllner K., *ET AL.*: 'Highly efficient transmission gratings in fused silica for chirped-pulse amplification systems', *Appl. Opt.*, 2003, **42**, pp. 6934–6938

[19] Franssila S.: 'Introduction to microfabrication' (Wiley, New York, 2004), p. 125

[20] Ferstl M.: 'Highly selective etching of deep silica components using electron cyclotron resonance plasma', *Microelecron. Eng.*, 2002, **61–62**, pp. 881–886

[21] Metwalli E., Pantano C.G.: 'Reactive ion etching of glasses: composition dependence', *Nucl. Instrum. Meth. Phys. Res. B*, 2003, **207**, pp. 21–27

[22] Chae H., Vitale S.A., Sawin H.H.: 'Silicon dioxide etching yield measurements with inductively coupled fluorocarbon plasmas', *J. Vac. Sci. Technol. A*, 2003, **21**, pp. 381–387

[23] Rodriguez I., Spicar-Mihalic P., Kuyper C.L., Fiorini G.S., Chiu D. T.: 'Rapid prototyping of glass microchannels', *Anal. Chim. Acta.*, 2003, **496**, pp. 205–215

[24] Li L., Esashi M., Abe T.: 'A miniaturized biconvex quartz-crystal microbalance with large-radius spherical thickness distribution', *Appl. Phys. Lett.*, 2004, **85**, pp. 2652–2654

[25] Goyal A., Hood V., Tadigadapa S.: 'High-speed anisotropic etching of quartz using SF6/C4F8/Ar/O2 based chemistry in inductively coupled plasma reactive ion etching system', *Proc. SPIE*, 2006, **6111**, p. 61110

[26] Li X., Ling L., Hua X., Fukasawa M., Oehrleinc G.S.: 'Effects of Ar and O_2 additives on SiO_2 etching in C4F8-based plasmas', *J. Vac. Sci. Technol. A*, 2003, **21**, pp. 284–293

[27] Jung H.K., Hwang Y.S., Hyeon I.J., Kim Y.K., Baek C.W.: 'Silicon/quartz bonding and quartz deep RIE for the fabrication of quartz resonator structures'. Proc. IEEE Int. Nano/Micro Eng. Mol. Syst. Conf., 2008, pp. 1172–1176

[28] Mohamed K., Alkaisi M.M.: 'Three-dimensional pattern transfer on quartz substrates', *Microelecron. Eng.*, 2010, **87**, pp. 1463–1466

[29] Chen H., Fu C.: 'An investigation into the characteristics of deep reactive ion etching of quartz using SU-8 as a mask', *J. Micromech. Microeng.*, 2008, **18**, p. 105001

doi: 10.1049/mnl.2014.0093